Comprehensive Survey On Remote Sensing Image Processing Techniques for Image Classification

Thuy Thi Tran[1] and Hiep Xuan Huynh[2(✉)]

[1] Faculty of Information Technology – Communication, University of CuuLong, Vinh Long, Vietnam
[2] College of Information and Communication Technology, Can Tho University, Can Tho, Vietnam
hxhiep@ctu.edu.vn

Abstract. Remote sensing technology is now being used with unprecedented high resolution, making important contributions in practical applications such as urban development, construction planning and disaster prediction. However, although many scholars have studied algorithms for remote sensing image processing, there have not been detailed summary articles to support new researchers in this field. In this paper, we present an overview of remote sensing images, types of remote sensing satellite images and related studies. Next, we briefly review the recent history of remote sensing image processing techniques. Then, list related studies on remote sensing image classification. Finally, based on the current status of research on remote sensing images, we propose some future research directions in order to provide survey references for new studies in the field of remote sensing.

Keywords: remote sensing · resolution · satellite sensors · classification · spatial point pattern

1 Introduction

Remote sensing is the process of gathering data about the earth's surface without being in contact with it [1]. This is process is done by sensing and recording emitted or reflected energy and then processing, analyzing and applying that information. Remote sensing process includes the illumination or energy source which passes through the atmosphere and interacts with the target; the electromagnetic energy emitted or scattered from the target is collected and recorded by the satellite sensors is transmitted in electronic form to a receiving and processing station where the data is processed into an image [2]. The processed image is interpreted visually or electronically or digitally to extract the information about the illuminated target. Remote sensing systems which measure reflected energy are called passive sensors, which can be used only to detect energy in the present of naturally occurring energy. This can take place only during the time when the sun is illuminating the earth [3].

P. Cong Vinh and N. Thanh Tung (Eds.): ICCASA 2023, LNICST 579, pp. 102–114, 2024.
https://doi.org/10.1007/978-3-031-58878-5_7

An active sensor provides its own energy source for illumination [2]. The sensors emit radiation which is directed towards the target to be investigated; these sensors obtain the information regardless of the time of day. In order to capture the earth's surface the sensors must be paced in a proper platform. Before it was ground-based and aircrafts platforms, nowadays satellite near-polar orbits platform provides a great contribution to remote sensing imagery.

The Multispectral satellite sensor provides digital raster images, that allow us to apply Digital Image Processing techniques to develop thematic maps of landuse/landcover classes which are essential in many remote sensing applications like forestry, agriculture, environmental studies, weather forecasting, ocean studies, archeological studies etc.

In this paper various advanced image processing techniques to convert raw satellite imagery into fine data obtained from different spatial, spectral and temporal resolutions from microwave to ultraviolet bands are discussed.

The paper is organized as follows; Sections 1, 2 deal with various resolutions of satellite sensor. Section 3 describes Satellite sensors for distinct applications. Sections 4, 5 is a study of Image Analysis which includes advance algorithms for preprocessing, enhancement, transformation and classification. Section 6 presents conclusion.

2 Remote Sensing Satellite Imagery

Remote sensing satellite image consists of Digital Numbers which represent image features such as color, brightness, wavelength, radiated energy frequency, or picture element in the image. The smallest element on an image is called pixel. A digital image consists of pixels which are arranged in rows and columns commonly known as a raster image. The information content and dimensions of these pixels depend on the resolution of the image. Figure 1 shows various sensor resolutions.

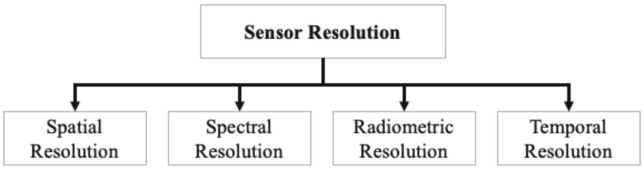

Fig. 1. Satellite Sensor Resolutions

2.1 Spatial Resolution

The detail of an image depends on spatial resolution of the sensor. If the spatial resolution is 10 m, it means that each pixel denotes an area of 10 m/10 m on the ground surface. Higher the resolution of an image, finer details is more clearly-visible and cover less ground area. Lower the resolution of an image, details are not clearly visible but it covers larger total ground area.

Yu Huang et al., [4] indicated that as the resolution decreases, the accuracy of landslide detection also decreases. The overall landslide area detection rate of UAV imagery

can reach 82.17%, while that of GF-6 and Landsat 8 imagery is only 52.26% and 48.71%. The landslide quantity detection rate of UAV imagery can reach 99.07%, while that of GF-6 and Landsat 8 images is only 48.71% and 61.05%. In addition, for each landslide detected, little difference is found in large-scale landslides, and it becomes more difficult to correctly detect small-scale landslides as the resolution decreases. For example, landslides under 100 m2 could not be detected from a Landsat 8 satellite image.

2.2 Spectral Resolution

Spectral resolution of a sensor is the ability to define fine wavelength intervals in an Electromagnetic spectrum. The details of an image also depend on responses of Electromagnetic Radiation incident on an object over distinct wavelength ranges, for example, the classification of vegetation and water is usually be separated in a broad wavelength range i.e., visible and near infrared wavelengths, to distinguish different rocks needs finer wavelength range within the band to separate them. So higher the spectral resolution, narrower the wavelengths range of a particular band.

Zou et al. [5] CCC-sensitive and MTA-insensitive satellite broadband vegetation indices are developed for crop canopy chlorophyll content estimation. The most efficient broadband vegetation indices for four satellite sensors (Sentinel-2, RapidEye, WorldView-2 and GaoFen-6) with red edge channels were identified (in the context of various vegetation index types) using simulated satellite broadband reflectance based on field measurements and validated with PROSAIL model simulations. The results indicate that developed vegetation indices present strong correlations with CCC and weak correlations with MTA, with overall R2 of 0.76–0.80 and 0.84–0.95 for CCC and R2 of 0.00 and 0.00–0.04 in the field measured data and model simulations, respectively. The best vegetation indices identified in this study are the soil-adjusted index type index SAI (B6, B7) for Sentinel-2, Verrelts's three-band spectral index type index BSI-V (NIR1, Red, Red Edge) for WorldView-2, Tian's three-band spectral index type index BSI-T (Red Edge, Green, NIR) for RapidEye and difference index type index DI (B6, B4) for GaoFen-6. The identified indices can potentially be used for crop CCC estimation across species and seasonality.

Zhang et al. [6] demonstrated a novel oceanic triple-field-of-view (FOV) high-spectral-resolution lidar (HSRL) with an iterative retrieval approach. This technique provides, for the first time, comprehensive, continuous, and vertical measurements of seawater absorption coefficient, scattering coefficient, and slope of particle size distribution, which are validated by simulations and field experiments. Furthermore, it depicts valuable application potentials in the accuracy improvement of seawater classification and the continuous estimation of depth-resolved particulate organic carbon export. The triple-FOV HSRL with high performance could greatly increase the knowledge of seawater constituents and promote the understanding of marine ecosystems and biogeochemistry.

2.3 Radiometric Resolution

Radiometric resolution enables us to recognize high and low level contrast objects in an image. Radiometric resolution describes the information about image brightness, contrast, illumination variations and other details of an image.

Verde et al. [7] concluded that high radiometric resolution data does not always lead to higher and more accurate classification results, although in certain cases the classification results of higher radiometric resolution data are more accurate than lower radiometric resolution data. The study ran experiments on remote sensing datasets with radiometric resolution at three different locations. The bagging classification method used gives low radiometric resolution. The study also confirmed that image content retrieval and processing time also depend on the radiometric resolution of the image. Experiments also showed no correlation between classification based on radiometric resolution and classification based on texture bands and spectral indices.

2.4 Temporal Resolution

The time taken by a satellite to revisit the same area with same viewing angle is referred as absolute temporal resolution. It refers to the length of time it takes for a satellite to complete one entire orbit cycle. Temporal data plays a very important role in remote sensing applications like monitoring vegetation changes, flood occurrence, deforestation, urban development etc., Spectral resolution varies with time and is identified by multi temporal imagery. Temporal resolution depends on many factors like satellite sensor capability, latitude and swath overlap.

Wang et al. [8] integrated multisource remote sensing, including satellite altimetry and optical and synthetic aperture radar (SAR) images, to generate weekly water levels and water storages of nine largest reservoirs on the main stem of the LMR from 2017 to 2021. Specifically, partial surface water extent (SWE) of reservoirs was extracted from Sentinel-1 SAR images and digital elevation models (DEMs), using Random Forest algorithms trained by partial SWE derived from Sentinel-2 optical images, showing an overall accuracy higher than 95%. Based on the partial SWE and water level estimates from ICESat-2 and Global Ecosystem Dynamics Investigation (GEDI, International Space Station-based) data, the relationships between water levels and partial SWE were derived to convert partial SWE into water level time series. Furthermore, water storage time series of the nine reservoirs were obtained from water level time series and hypsometric functions derived from SRTM DEMs that were corrected by ICESat-2 data to remove systematic errors. For the Xiaowan Reservoir on the Lancang River, there is close agreement between remote sensing-derived water levels and in-situ water levels in terms of a normalized RMSE lower than 5%. Results indicate that multisource remote sensing has large potential for high-temporal-resolution monitoring of reservoir water levels and water storage.

3 Satellite Sensors

Satellites provide remote sensing imagery which are commonly used today. The unique characteristics of Satellites make them particularly useful for remote sensing of the Earth's surface.

3.1 Thermal Sensors

To measure the surface temperature and thermal properties of a target object on the ground surface, thermal sensors are used that detects the reflected radiation from the target object.

Further contributions to research in the field of land surface temperature (LST) calculation using low-altitude thermal infrared (TIR) remote sensing image data. Yafei Wu et al. [9] evaluated the small-scale urban thermal environment by proposing a block-scale land surface temperature retrieval model with high spatial and thermal resolution. Experimental data using multi-source remote sensing images. The results were compared with the land surface temperature measured in the field area with the proposed model's accuracy of 0.09K. The results of the study can be used to quantitatively analyze land surface temperature patterns in urban areas at the block scale.

3.2 Airborne and Space-Borne Sensors

Airborne remote sensing are one time operations. Here, sensors are mounted on air-crafts that provides images with high spatial resolution but it covers less ground area. Space-borne remote sensing provides continuous monitoring of earth's surface. Here, the sensors are placed on space shuttles or satellites. It covers larger earth's surface with less spatial resolution.

Hirschmugl et al. [10], evaluated forest structure based on spaceborne and airborne Lidar data in a natural forest in an Austrian Alp. Data to run waveform experiments. Number of layers and foliage height height diversity are two indicators that have been used to explain the vertical structure of natural forests. In general, the overall accuracy of the research results is affected by natural forests with high vertical structures and rugged terrain. However, this is also a study that can provide future research directions on assessing forest structure using waveform data. Future studies can run experiments on managed forest areas with a simpler structure to reevaluate the parameters used in forest structure analysis, foliage height and number of layers.

This study [11] conducted a quantitative retrieval and validation of the Leaf Area Index (LAI) profiles using terrestrial and airborne laser scanning (TLS and ALS) and spaceborne GEDI data over a deciduous needleleaf forest site in northern China. The vertical LAI profile was estimated in the field using an upward digital hemispherical photography (DHP) attached to a portable measurement system in 2020 and 2021. A suite of new LiDAR indices combining both LiDAR return number and return intensity was explored for the LAI profile estimation. All LAI profiles obtained from the DHP, TLS, ALS, and GEDI during the leaf-on season and leaf-off season were compared. The DHP shows a good agreement with the TLS LAI profiles ($R2 = 0.97$). The LAI profile derived from the ALS data using the combined light penetration index (LPIRI) agrees well ($R2 \geq 0.86$) with the DHP, TLS, and GEDI estimates. In general, the LPIRI is advantageous for regional LAI profile mapping from ALS. The GEDI cumulative LAI corresponds well with the DHP during the leaf-on season ($R2 = 0.90$, $RMSE = 0.23$), but underestimates during the leaf-off season ($R2 = 0.70$, $RMSE = 0.14$, $bias = -0.13$). The underestimation is attributed to the higher canopy and ground reflectance ratio ($\rho v/\rho g$) assigned in the algorithm and the height discrepancy between the GEDI and field

measurements. For the GEDI LAI profile product, further validation and improvement are necessary for other biome types and landscape conditions, especially during the leaf-off season.

4 Image Analysis

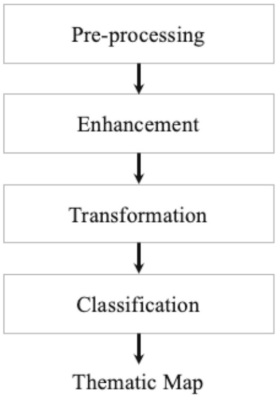

Fig. 2. Remote Sensing Analysis

In order to make good use of remote sensing data, we must be able to extract meaningful information from the image by applying proper processing techniques. Remote sensing images can also be represented in a computer as arrays of pixels, with each pixel corresponding to a digital number [DN], represents the brightness level of that pixel in an image. Figure 2 is a general architecture of remote sensing image analysis.

Image analysis systems can be categorized into following: (i) Pre-processing, (ii) Image Enhancement, (iii) Image Transformation, (iv) Image Classification and Analysis.

4.1 Pre-processing

Pre-processing functions involves the operations required prior to the main data analysis and consists of processes aimed at geometric correction, radiometric correction and atmospheric corrections to improve the ability to interpret the image components qualitatively and quantitatively. These process correct the data for sensor irregularities and removing (radiometric corrections) unwanted sensor distortion or atmospheric noise.

According to the imaging characteristics of Night time light (NTL) images, this paper [12] proposes to take high-precision road network data as geometric reference, extract control points by automatic matching between NTL images and road network data, and then realize geometric correction of NTL images. Taking the Luojia 1 -01 (LJ 1–01) satellite NTL image as an example, the experimental verification shows that the accuracy of geometric correction based on road network control can reach the sub-pixel level, which verifies the feasibility of the proposed method. This paper verifies the

rationality of using the road network as the benchmark data for NTL images, provides a feasible idea for subsequent scholars to study the geometric processing of NTL images, and ensures the geometric quality of data for the application of multi-temporal NTL images.

Homomorphic filtering is employed to enhance thermal infrared (TIR) image details and the modified RIFT algorithm is proposed to achieve TIR-visible image registration [13]. Different from using MIM for feature description in RIFT, the proposed modified RIFT uses the novel binary pattern string to descriptor construction. With sufficient and uniformly distributed ground control points, the two-step orthorectification framework, from SDGSAT-1 TIS L1A image to L4 orthoimage, are proposed in this study. The first experiment, with six TIR-visible image pairs, captured in different landforms, is performed to verify the registration performance, and the result indicates that the homomorphic filtering and modified RIFT greatly increase the number of corresponding points. The second experiment, with one scene of an SDGSAT-1 TIS image, is executed to test the proposed orthorectification framework. Subsequently, 52 GCPs are selected manually to evaluate the orthorectification accuracy. The result indicates that the proposed orthorectification framework is helpful to improve the geometric accuracy and guarantee for the subsequent thermal infrared applications.

Radiometric correction is one of the most important preprocessing parts of unmanned aerial vehicle (UAV) multispectral remote sensing data analysis and application [14]. In this article, a back propagation (BP) neural network-based radiometric correction method (BPNNRCM) considering optimal parameters was proposed. In the aspect of accuracy and robustness, the absolute errors of test and cross-validation images' surface reflectance obtained by the BPNNRCM were all less than 0.054. The BPNNRCM had smaller average absolute error (0.0141), mean squared error (0.0003), mean absolute error (0.0141) and mean relative error (7.1%) comparing with empirical line method and radiative transfer model.

Pahlevan et al. [15] summarize their results using performance matrices guiding the satellite user community through the Optical Water Types specific relative performance of Atmospheric correction processors. Their analysis stresses the need for better representation of aerosols, particularly absorbing ones, and improvements in corrections for sky- (or sun-) glint and adjacency effects, in order to achieve higher quality downstream products in freshwater and coastal ecosystems.

Quinten et al. [16], proposed a dark spectrum fitting (DSF) atmospheric correction model based on high-resolution optical remote sensing images such as Sentinel-2 and Landsat, for underwater applications. The model includes two processing processes: image brightness correction and automatic layering of panoramic images. The proposed solution used multiple dark targets in the secondary scene to construct a dark spectral range used to estimate atmospheric path reflectance based on the best-fit aerosol model. This model is completely automatic so it can be used to process the entire study area, specifically the North Sea. DSF will select the most appropriate range to overcome the problem of amplifying lighting effects in atmospheric correction. From the SWIR bands, the reflectance of sunlight can be estimated for calibration and use in low areas such as deep sea.

4.2 Enhancement

To make image easier for visual interpretation Enhancements are used. The advantage of digital imagery is that it allows us to manipulate the digital pixel values in an image. Although radiometric corrections for illumination, atmospheric influences, and sensor characteristics may be done prior to distribution of data to the user, the image may still not be optimized for visual interpretation. Image Enhancement methods are of four types: (i) Radiometric Enhancement; (ii) Spatial Enhancement; (iii) Spectral Enhancement; (iv) Geometric Enhancement.

One of the major disadvantages of waveform airborne laser scanners is the loss of signal strength of the data due to the path of the laser pulse through objects such as tree canopies or buildings. Richter et al., [17] proposed a model for radiometric enhancement of full-waveform airborne laser scanner data. This research can be used in environmental applications to represent the volume of objects that need to be studied. Another important contribution of the study is the ability to provide information about the structure of plants using radiometric enhancement techniques of airborne laser scanners.

Yang et al., [18] proposed a new model based on spatially enhanced UNet to handle the global road network by combining dense connection points and spatial convolutional neural network. The proposed solution is the integration of a structural conservation model and previously collected road surface information to be able to predict successive events in space. Experimental results have shown that the proposed solution has better performance than previous road solutions.

This article [19] reviews and discusses the most important algorithms relevant to this area of research between 2002 and 2022, along with the most frequently used datasets, HSI sensors, and quality metrics. Metaanalysis are drawn based on the aforementioned information, which is used as a foundation that summarizes the state of the field in a way that bridges the past and the present, identifies the current gap in it, and recommends possible future directions.

The geometric enhancement of the OpenStreetMap (OSM) road network using a standard national map as a reference. Belhouari et al., [20] use two transformation methods, the global transformation and the local transformation. The application of this approach in the geometric enhancement / correction where each node of the OSM network will have a newly calculated position. Both approaches have been tested in the region of Oran in Algeria as testing example.

4.3 Transformation

Image transformations typically involve the manipulation of multiple bands of data, whether from a single multispectral image or from two or more images of the same area acquired at different times (i.e. multitemporal image data). Either way, image transformations generate new images from two or more sources that highlight particular features or properties of interest, better than the original input images. Image transformation includes basic arithmetic operations like band Arithmetic operations are performed on two or more co- registered images of same geographical area. They may have different spectral band from a single multispectral data or it may have individual band of different time series data set.

The spectral transformation highlighted the characteristics of spectral curves and improved the relationship between spectral reflectance and anthocyanin, and the remote sensing model based on the first-order differential spectrum portrayed the best estimation accuracy (R2c = 0.91; R2v = 0.51) [21].

Zhang et al., [22] improved the remote sensing-based soil salinity content extraction from the Landsat 8, Digital elevation model and HJ-1A CCD satellite data using the Cuckoo Search Algorithms-Support Vector Machines model. The analysis of soil and vegetation factors shows that the first three principal components cumulative variance contributed 99.69% on the raw remote sensing image, while the first two principal components cumulative variance contributed 88.01% and 85.28% on the first- and second-order differential transformation remote sensing images, respectively.

5 Image Classification and Analysis

Image classification is an important part of the remote sensing, image analysis and pattern recognition. Based on the idea that different feature types on the earth's surface have a different spectral reflectance and remittance properties, their recognition is carried out through the classification process.

This study [23] presented the performance of the Mangrove Vegetation Index (MVI) and image classification algorithms, embedded in the Google Earth Engine, applied to Landsat-8 and Sentinel-2 data, to map tracts of mangroves in Aracaju (Sergipe, Brazil). Results reveal that the Cobweb clustering algorithm applied to MVIderived from Landsat-8 data favors reliable and practical mangrove mapping, considering the broad diversity of vegetation conditions in this habitat.

To improve the global cloud detection performance for Landsat satellite imagery, Pang et al., [24] used a combination of convolutional neural network models. Landsat satellite imagery provides discrete spectral channels from short wavelengths (green, blue, red) to visible infrared wavelengths through its surface radiometric sensors of objects on Earth. The experimental results were re-evaluated with the Landsat 8 Bio dataset and it was determined that the cloud of the extended UNet model had the best results among the estimated models.

This review [25] provided an overview of Earth Observation data, machine learning and state-of-the-art deep learning techniques that are currently being used to quantify above-ground carbon, below-ground carbon, and soil carbon stocks of mangroves, seagrasses and saltmarshes ecosystems. Some key limitations and future directions for the potential use of data fusion combined with advanced machine learning, deep learning, and metaheuristic optimisation techniques for quantifying blue carbon stocks are also highlighted. In summary, the quantification of blue carbon using remote sensing and machine learning approaches holds great potential in contributing to global efforts towards mitigating climate change and protecting coastal ecosystems.

The urbanization process greatly affects the global warming process. The identification of urban areas plays an increasingly important role. One of the solutions that is continuous in space and time and has a low cost to support this problem is to use remote sensing images. Chen et al., [26] used Landsat 8 satellite images to extract information about land surface temperature, combined with OpenStreetMap to locate urban areas,

using point of interest to determine the data area that needs attention for processing. A deep learning algorithm is a random forest used to re-evaluate urban areas with respect to the temperature environment of the land surface. The assessment results are correct for areas along the Hunhe River with gradually decreasing land surface temperatures, and higher temperatures in urban central areas. From the results of this study, future researchers in the field of processing land surface temperature from remote sensing images can do further research to provide results to support functional sectors in the process of urbanization in a reasonable way to combat climate change.

Deep Convolutional Embedded Clustering (DCEC) is a new unsupervised deep learning method, which was used by Maarten et al., [27] to generate a landscape typology for Switzerland. This method encodes the input image into a hidden layer. This hidden layer is used to classify images into separate clusters such as demographic classes, terrain, flora and fauna ecology, etc. The results of the study were successfully run experiments to distinguish 45 types of continuous landscapes with input data from remote sensing images. This is a promising solution for future researchers in the field of land systems, geology and landscape classification.

The focus of this study [28] was to investigate the application of hyperspectral remote sensing and deep learning (DL) for real-time ore and waste classification. Hyperspectral images of several meters of drill core samples from a silver ore deposit labeled by a site geologist as ore and waste material were used to train and test the models. A DL model was trained on the labels generated by a spectral angle mapper (SAM) machine learning technique. The performance on ore/waste discrimination of three classifiers (supervised DL and SAM, and unsupervised k-means clustering) was evaluated using Rand Error and Pixel Error as disagreement analysis and accuracy assessment indices. The results showed that the DL method outperformed the other two techniques. The performance of the DL model reached 0.89, 0.95, 0.89, and 0.91, respectively, on overall accuracy, precision, recall, and F1 score, which indicate the strong capability of the DL model in ore and waste discrimination. An integrated hyperspectral imaging and DL technique has strong potential to be used for practical and efficient discrimination of ore and waste in a near real-time manner.

Xu et al., [29] proposed an unsupervised domain adaptation model to solve the difficulty caused by the large distribution difference between the source and target domains. The purpose of the proposed model is that during the conversion process, it is necessary to keep the data in the source domain intact for classification in the target domain, especially for unlabeled data.

Classification methods based on thresholds of vegetation indices do not accurately estimate the flooded area in areas with heterogeneous water surfaces. Foroughnia et al., [30] used synthetic aperture radar and multispectral data and machine learning methods for unsupervised and supervised classification to classify flooded areas. This solution overcame problems with water clarity and emerging vegetation.

Stromann et al., [31] used the computational power of Google Earth Engine and Google Cloud Platform to generate an oversized feature set in which we explore feature

importance and analyze the influence of dimensionality reduction methods to object-based land cover classification with Support Vector Machines. They propose a methodology to extract the most relevant features and optimize an SVM classifier hyperparameters to achieve higher classification accuracy. The proposed approach is evaluated in two different urban study areas of Stockholm and Beijing. Despite different training set sizes in the two study sites, the averaged feature importance ranking showed similar results for the top-ranking features. In particular, Sentinel-2 NDVI, NDWI, and Sentinel-1 VV temporal means are the highest ranked features and the experiment results strongly indicated that the fusion of these features improved the separability between urban land cover and land use classes. Overall classification accuracies of 94% and 93% were achieved in Stockholm and Beijing study sites, respectively. The test demonstrated the viability of the methodology in a cloud-computing environment to incorporate dimensionality reduction as a key step in the land cover classification process, which they consider essential for the exploitation of the growing Earth observation big data.

6 Conclusion

Remote sensing is going mainstream, both in the business and personal worlds, and has the potential to lead us into the metaverse. Within the framework of this article, 31 articles have been selected and analyzed, including different cases of resolution, sensing of remote sensing images, analysis and classification of remote sensing images. Particular emphasis is placed on the various machine learning methods (supervised and unsupervised) adopted by the research community in conjunction with Earth Observation data, used as well as problem statements. The general comment of this study is that there is no standardized approach to general application for remote sensing image processing to bring the most optimal efficiency. We propose spatial point pattern approaches to further improve the accuracy, efficiency, and applicability of remote sensing image classification in the combination of computer science and business. Specifically, we use the spatial point pattern technique to classify the locations of restaurants, hotels or residential areas so that investors can strategically deploy a retail agency system with appropriate locations to improve business efficiency as much as possible.

References

1. Gibson, P.J., Power, C.H., Keating, J.: Introductory Remote Sensing: Principles and Concepts. Routledge (2013). https://doi.org/10.4324/9780203714522
2. Richards, J A.: Remote Sensing Digital Image Analysis, Sixth Edition, Springer (2022).
3. Revanna, S., Deepa, P., Venugopal, K.R.: Remote sensing satellite image processing techniques for image classification. Int. J. Comput. Appl. **161**, 24–37 (2017). https://doi.org/10.5120/ijca2017913306
4. Huang, Y., et al.: How spatial resolution of remote sensing image affects earthquake triggered landslide detection: an example from 2022 luding earthquake, Sichuan, China. Land **12**, 681 (2023). https://doi.org/10.3390/land12030681
5. Zou, X., Jin, J., Mõttus, M.: Potential of satellite spectral resolution vegetation indices for estimation of canopy chlorophyll content of field crops: mitigating effects of leaf angle distribution. Remote Sens. **15**, 1234 (2023). https://doi.org/10.3390/rs15051234

6. Zhang, K., et al.: Comprehensive, continuous, and vertical measurements of seawater constituents with triple-field-of view high-spectral-resolution lidar. Research**6**, 0201 (2023) https://doi.org/10.34133/research.0201
7. Verde, N., Mallinis, G., Tsakiri-Strati, M., Georgiadis, C., Patias, P.: Assessment of radiometric resolution impact on remote sensing data classification accuracy. Remote Sens. **10**, 1267 (2018). https://doi.org/10.3390/rs10081267
8. Wang, Y., Long, D., Li, X.: High-temporal-resolution monitoring of reservoir water storage of the Lancang-Mekong River. Remote Sens. Environ. **292**, 113575 (2023). https://doi.org/10.1016/j.rse.2023.113575
9. Wu, Y., Shan, Y., Lai, Y., Zhou, S.: Method of calculating land surface temperatures based on the low-altitude UAV thermal infrared remote sensing data and the near-ground meteorological data. Sustain. Cities Soc. **78**, 103615 (2022). https://doi.org/10.1016/j.scs.2021.103615
10. Hirschmugl, M., Lippl, F., Sobe, C.: Assessing the vertical structure of forests using airborne and spaceborne LiDAR data in the Austrian alps. Remote Sens. **15**, 664 (2023). https://doi.org/10.3390/rs15030664
11. Wang, Y., Fang, H., Zhang, Y., Li, S., Pang, Y., Ma, T.: Retrieval and validation of vertical LAI profile derived from airborne and spaceborne LiDAR data at a deciduous needleleaf forest site. GISci. Remote Sens. **60**(1) (2023) https://doi.org/10.1080/15481603.2023.2214987
12. Zhang, L., Zhang, G., Liu, W., Li, Z., Xie, T.: Geometric correction of Luojia 1-01 nighttime light image based on road network. J. Imaging Sci. Technol. **67**(2), 1–12 (2023). https://doi.org/10.2352/J.ImagingSci.Technol.2023.67.2.020401
13. Chen, J., et al.: A TIR-visible automatic registration and geometric correction method for SDGSAT-1 thermal infrared image based on modified RIFT. Remote Sens. **14**, 1393 (2022). https://doi.org/10.3390/rs14061393
14. Zhang, Y., et al.: A back propagation neural network-based radiometric correction method (BPNNRCM) for UAV multispectral image. IEEE J. Sel. Top. Appl. Earth Observations Remote Sens. **16**, 112–125 (2023). https://doi.org/10.1109/JSTARS.2022.3223781
15. Pahlevan, N., et al.: ACIX-Aqua: A global assessment of atmospheric correction methods for Landsat-8 and Sentinel-2 over lakes, rivers, and coastal waters. Remote Sens. Environ. **258**, 112366 (2021). https://doi.org/10.1016/j.rse.2021.112366
16. Vanhellemont, Q.: Adaptation of the dark spectrum fitting atmospheric correction for aquatic applications of the landsat and sentinel-2 archives. Remote Sens. Environ. **225**, 175–192 (2019). https://doi.org/10.1016/j.rse.2019.03.010
17. Richter, K., Maas, H.-G.: Radiometric enhancement of full-waveform airborne laser scanner data for volumetric representation in environmental applications. ISPRS J. Photogramm. Remote Sens. **183**, 510–524 (2022). https://doi.org/10.1016/j.isprsjprs.2021.10.021
18. Yang, M., Yuan, Y., Liu, G.: SDUNet: road extraction via spatial enhanced and densely connected UNet. Pattern Recogn. **126**, 108549 (2022). https://doi.org/10.1016/j.patcog.2022.108549
19. Aburaed, N., Alkhatib, M.Q., Marshall, S., Zabalza, J., Ahmad, H.A.: A review of spatial enhancement of hyperspectral remote sensing imaging techniques. IEEE J. Sel. Top. Appl. Earth Observations Remote Sens. **16**, 2275–2300 (2023). https://doi.org/10.1109/JSTARS.2023.3242048
20. Belhouari, F.Z., Boukerch, I., Siyoucef, K.: Geometric Enhancement of the openstreetmap road network. ISPRS Ann. Photogrammetry Remote Sens. Spat. Inf. Sci. **V-4–2021**, 33–39 (2021). https://doi.org/10.5194/isprs-annals-V-4-2021-33-2021
21. Luo, L., Chang, Q., Gao, Y., Jiang, D., Li, F.: Combining different transformations of ground hyperspectral data with unmanned aerial vehicle (UAV) images for anthocyanin estimation in tree peony leaves. Remote Sens. **14**, 2271 (2022). https://doi.org/10.3390/rs14092271

22. Zhang, F., et al.: Retrieval of soil salinity based on multi-source remote sensing data and differential transformation technology. Int. J. Remote Sens. **44**(4), 1348–1368 (2023). https://doi.org/10.1080/01431161.2023.2179900
23. Rodrigues, F., de Souza Filho, C.R., Del Papa, R., Scafutto, M., Lassalle, G.: Mangrove mapping strategies using google earth engine and landsat8 and sentinel-2 imagery data, Anais do Simposio Brasileiro de Sensoriamento Remoto (2023)
24. Pang, S., Sun, L., Tian, Y., Ma, Y., Wei, J.: Convolutional neural network-driven improvements in global cloud detection for landsat 8 and transfer learning on sentinel-2 imagery. Remote Sens. **15**, 1706 (2023). https://doi.org/10.3390/rs15061706
25. Pham, T.D., et al.: Advances in Earth observation and machine learning for quantifying blue carbon. Earth Sci. Rev. **243**, 104501 (2023). https://doi.org/10.1016/j.earscirev.2023.104501
26. Chen, Y., Yang, J., Yang, R., Xiao, X., Xia, J.C.: Contribution of urban functional zones to the spatial distribution of urban thermal environment. Build. Environ. **216**, 109000 (2022). https://doi.org/10.1016/j.buildenv.2022.109000
27. van Strien, M.J., Grêt-Regamey, A.: Unsupervised deep learning of landscape typologies from remote sensing images and other continuous spatial data. Environ. Model. Softw. **155** (2022) https://doi.org/10.1016/j.envsoft.2022.105462
28. Abdolmaleki, M., Consens, M., Esmaeili, K.: Ore-waste discrimination using supervised and unsupervised classification of hyperspectral images. Remote Sens. **14**, 6386 (2022). https://doi.org/10.3390/rs14246386
29. Xu, M., Wu, M., Chen, K., Zhang, C., Guo, J.: The eyes of the gods: a survey of unsupervised domain adaptation methods based on remote sensing data. Remote Sens. **14**, 4380 (2022). https://doi.org/10.3390/rs14174380
30. Foroughnia, F., Alfieri, S.M., Menenti, M., Lindenbergh, R.: Evaluation of SAR and optical data for flood delineation using supervised and unsupervised classification. Remote Sens. **14**, 3718 (2022). https://doi.org/10.3390/rs14153718
31. Stromann, O., Nascetti, A., Yousif, O., Ban, Y.: Dimensionality reduction and feature selection for object-based land cover classification based on sentinel-1 and sentinel-2 time series using google earth engine. Remote Sens. **12**, 76 (2020). https://doi.org/10.3390/rs12010076